

Biogenic Synthesis of Silver Nanoparticles Using Fruit Aqueous Extract of *Psidium Guajava* and Its Antibacterial Activity

Babak Sadeghi^{1*}, Bitakoupaei¹

¹ Department of Chemistry, Tonekabon Branch, Islamic Azad University, Tonekabon, Iran

Received: 2017-05-08

Accepted: 2017-07-11

Published: 2017-08-20

ABSTRACT

One plant seed extract (*Psidium guajava*) was screened for their bioreduction behavior for synthesis of silver nanoparticles. *Psidium guajava* (PG) was found to exhibit the good reducing and protecting action in terms of synthesis rate and monodispersity of the prepared silver nanoparticles. UV-visible spectroscopy, X-ray diffraction (XRD), Fourier transform infrared spectroscopy (FTIR), transmission electron microscopy (TEM), scanning electron microscopy (SEM), and X-ray energy dispersive spectrophotometer (EDAX) was performed to ascertain the formation of Ag-NPs. Our measurements indicate that biosynthesis of Ag nanoparticles by *Psidium guajava* (PG) produces Ag nanoparticles with the diameters in the range of 30-36 nm. XRD studies reveal a high degree of crystallinity and monophasic Ag nanoparticles of face-centered cubic (FCC) structure. The FTIR result clearly showed that the extracts containing OH as a functional group act in capping the nanoparticles synthesis. Antibacterial activities of Ag-NPs were tested against the growth of Gram-positive (*S. aureus*) using SEM. The inhibition was observed in the Ag-NPs against *S. aureus*. The results suggest that the synthesized Ag-NPs act as an effective antibacterial agent. It is confirmed that Ag-NPs are capable of rendering high antibacterial efficacy and hence has a great potential in the preparation of drugs used against bacterial diseases.

Keywords: Silver nanoparticles; Green chemistry; Scanning electron microscopy (SEM); *Psidium guajava*; Antibacterial

© 2017 Published by Journal of Nanoanalysis.

How to cite this article

Sadeghi B, koupaei B. Biogenic Synthesis of Silver Nanoparticles Using Fruit Aqueous Extract of *Psidium Guajava* and Its Antibacterial Activity. J. Nanoanalysis., 2017; 4(2): 126-133. DOI: [10.22034/jna.2017.02.005](https://doi.org/10.22034/jna.2017.02.005)

INTRODUCTION

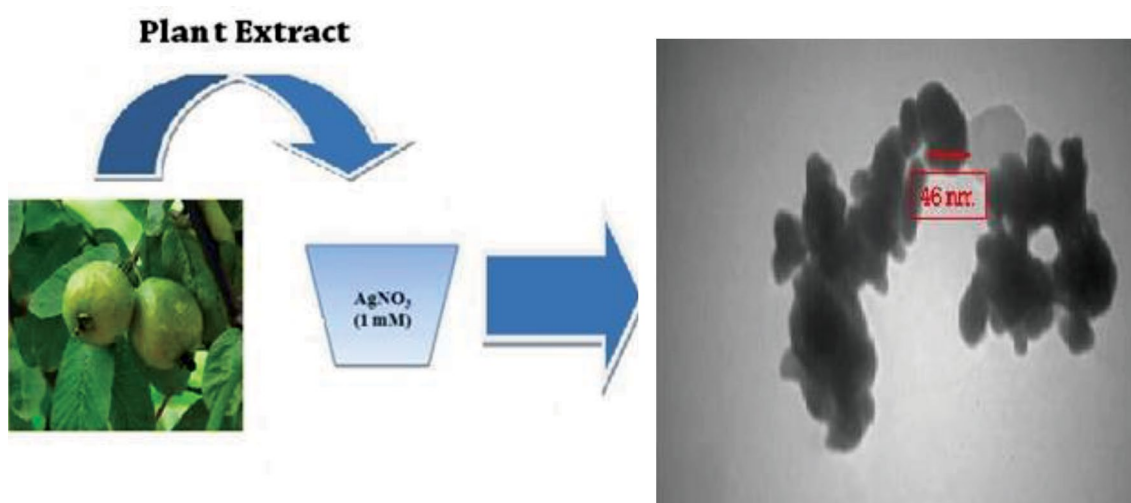
Nanotechnology is expected to be the basis of many of the main technological innovations of the 21st century Research and development. Plant extracts may act both as reducing agents and stabilizing agents in the synthesis of nanoparticles [1]. Silver nanoparticles have attracted the attention of the researchers in the

last two decades due to their wide applications in various fields. Nanotechnology is a broad interdisciplinary area of research, development and industrial activity which has been growing rapidly worldwide for the past decade. Metallic nanoparticles of specific sizes and morphologies can be readily synthesized using chemical and physical methods [1-5]. The literature is replete with the investigations of the use of plant extracts [6], fungi [7], alpha [8], proteins and enzymes [9] as the reductant for carrying out

* Corresponding Author Emails: b_sadeghi@toniau.ac.ir; bsadeghi1177@gmail.com
Tel: +98 (912)2898500, Fax: +98 (11)54270512

the syntheses of nanoparticles with a variety of shapes and morphologies in high yields, including multi-branched advanced silver and/or gold nanomaterials [10]; but the use of surfactant in the green synthesis of silver sol has been neglected. Most of the methods reported in the literature are extremely expensive and they also involve the use of toxic, hazardous chemicals as the stabilizers which may pose potential environmental and biological risks. Because of the increasing environmental concerns by chemical synthesis routes, an environmentally sustainable synthesis process has led to biomimetic approaches, which refers to applying biological principles in materials formation. Bio-reduction is one of the fundamental processes in the biomimetic synthesis. The stability, shape, size, and morphologies of metal nanoparticles strongly depend on the method of preparation, type, nature of reductants, and concentration of stabilizers (polymers, ligands, solid matrix and surfactants) [11]. The surface plasmon resonance and large effective scattering cross section of individual silver nanoparticles make them ideal candidates for molecular labeling where phenomena such as surface enhanced Raman scattering (SERS) can be exploited [12]. In addition, silver nanoparticles play a significant role in the field of biology and medicine due to its attractive physiochemical properties. The strong toxicity of silver against a wide range of microorganisms is well known and silver nanoparticles have been recently

shown to be a promising antimicrobial material [13–17]. Silver nanoparticles have found to possess anti-inflammatory, antiviral, anti-angiogenesis, and anti-platelet activity and cytotoxicity against cancer cells which makes them vital [18–20]. However, these methods employ toxic chemicals as reducing agents, or nonbiodegradable stabilizing agents and are therefore potentially dangerous to the environment and biological systems [21]. Moreover, most of these methods entail intricate controls or nonstandard. We have recently developed a reduction method of converting Ag nanospheres into nanorods [22], nanoplates [23], their antibacterial activity [24, 25], an improved an easy synthetic route for silver nanoparticles in poly (diallyldimethylammonium chloride) (PDDA) [26], synthesis of Gold/HPC hybrid nanocomposite [27], Preparation of ZnO/Ag nanocomposite [28] and comparison nanosilver particles and nanosilver plates for the oxidation of ascorbic acid [29]. Regarding the role of green chemistry, it was successfully demonstrated that size, shape and the antibacterial activity silver nanoparticles by the reduction of Ag^+ ions with bio-reductants (*Pistacia atlantica*) largely depend on the nature of reducing agents, concentration and time of mixing of the reactants [30]. The methodology employed here is very simple, easy to perform, inexpensive, and eco-friendly. Moreover, most of these methods entail intricate controls or nonstandard (Scheme 1).



Scheme 1. *Psidium guajava* (PG) fruit extract reduces and stabilizes Ag nanoparticles.

MATERIAL AND METHODS

Materials

Silver nitrate (AgNO_3) was obtained from Loba Chemie, India and used as received. All other reagents used in the reaction were of analytical grade with maximum purity. *Psidium guajava* (PG) fruit was collected from South of IRAN, and were cleaned with double distilled water and shade-dried for a week at room temperature and further (PG) fruit were ground to powder and stored for further study. For this experiment, nanoparticles have concentrations ranging from 0.0976 to 100 $\mu\text{g}/\text{mL}$. *S. Areas* (ATCC 51153) were used as a Gram-positive bacterium. For the antimicrobial activity measurement, bacteria cultures were incubated at 38 °C in Luria medium (tryptone 1.5%, yeast extract 0.75% sodium chloride 1.2%, agar 1%, Difco).

Synthesis and characterization of silver nanoparticles (Ag-NPs)

2 g of dried extract of *Psidium guajava* (PG) fruit is added into 25 ml deionized water in a conical flask along with 2 mL of methanol (minimum methanol was added in order to initiate the isolation of compounds). Then stirred for 1 h in a magnetic stirrer at room temperature. The extract was placed in a orbital shaker for 1 h and the extract was filtered. For the synthesis of silver nanoparticles various concentrations of leaf extracts were tried and then the extract to be used was optimized to 1 mL. Further, 1 mL of the extract was added to 10 mL of 1 mM silver nitrate (AgNO_3) solution and the solution was placed in orbital shaker at room temperature, for reduction of Ag^+ to Ag^0 . The broth containing Ag-NPs was centrifuged at 10,000 rpm for 15 min, following which the pellet was re-dispersed in the sterile distilled water to get rid of any uncoordinated biological molecules. The color change involved in the formation of silver nanoparticles. The purified pellets were then kept into petri plates and left in the oven for drying at 60 °C for 24 h. The colorless AgNO_3 solution turned yellow to brown or reddish yellow to deep red, indicated the formation of Ag-NPs. The dried Ag-NPs were scrapped out for the further study.

Antimicrobial activity studies

S. Areas (ATCC 51153) were used as a Gram-positive bacterium. For the antimicrobial activity measurement, bacteria cultures were incubated at 38° C in Luria medium (tryptone 1.5%, yeast extract 0.75%, sodium chloride 1.2%, agar 1%, Difco).

Antimicrobial activities of silver nanoparticles (Ag-NPs) have been investigated against *S. aureus* as the model Gram-positive bacteria. The in vitro anti-bacterial activities of silver nanoparticles were examined according Melaiye and Feng [31–33]. The following microorganism was used: Gram-positive *Staphylococcus aureus*.

Characterization of silver nanoparticles (Ag-NPs)

Nanoparticles are generally characterized by their size, shape, surface area, and dispersed [32–33]. The biosynthesis of the Ag-NPs in a solution was monitored by measuring the UV–vis spectra of the solutions (1:4 diluted) of the reaction mixture. UV–vis spectra were recorded on a double beam spectrophotometer (Shimadzu, model UV-1800, Kyoto, Japan) from 300 to 800 nm at a resolution of 1 nm. The distilled water was used as a blank. The Ag-NPs synthesized with 8% fruit extracts and 6 mM AgNO_3 solution were characterized with the help of scanning electron microscopy (model LEO 440i) equipped with X-ray energy dispersive spectrometer (EDAX) (Bankar et al., 2010). Transmission electron microscopy (TEM) selected area electron diffraction (SAED) images were taken on Zeiss - EM10C - 80 KV operated at accelerating voltages of 40 and 200 kV. The observed reflection planes corresponding to fcc Ag-NPs (~27 nm) in XRD diffraction pattern (Seisert Argon 3003 PTC uses nickel filtered XD-3Cu K α radiations ($k=1.5418 \text{ \AA}$)). The purified powders of Ag-NPs were subjected to FTIR spectroscopy (FTIR; Bomem MB100). These measurements were carried out on a Perkin-Elmer Spectrum-One instrument in the diffuse reflectance mode at a resolution of 4 cm^{-1} in KBr pellets. For comparison, a drop of 8% fruit extracts was mixed with KBr powder and palletized after drying properly. The pellets were later subjected to FTIR spectroscopy measurement.

RESULT AND DISCUSSION

UV–vis spectral studies

Light wavelengths in the 300–800 nm are generally used for characterizing various metal nanoparticles in the size range of 2 to 100 nm UV–vis spectroscopy was ascertained to check the formation and stability of Ag-NPs in aqueous solution (Fig.1.) [34]. The colorless AgNO_3 solution turned yellow to brown or reddish yellow to deep red, indicated the formation of Ag-NPs. The appearance of the brown color was due to the excitation of the surface plasmon resonance (SPR),

typical of Ag-NPs having λ_{\max} values which were reported earlier in the visible range of 450–470 nm [34] (Fig.1.). The SPR observance was extremely sensitive to the nature, size and shape of the particles formed and their inter particle.

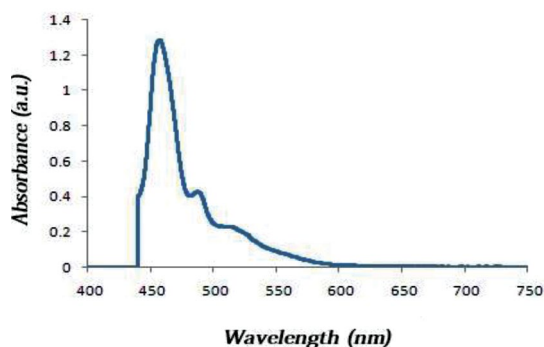


Fig. 1. UV-vis spectra of an aqueous solution of *Psidium guajava* (PG) fruit extract in presence of Ag^+ ions at 30°C . Reaction conditions: $[\text{Ag}^+] = 10.0 \times 10^{-4} \text{ mol dm}^{-3}$.

FTIR studies

FTIR analysis was used for the characterization of the extract and the synthesized nanoparticles (Fig.1). FTIR measurements were carried out to identify the possible biomolecules responsible for reduction, capping and efficient stabilization of the Ag nanoparticles. *Psidium guajava* (PG) is rich in proteins and have high availability of the amino acids [35]. The representative FTIR spectra of the control extract and (PG) and stabilized silver nanoparticles were shown in Fig. 2. It can be seen that, in contrast to the control (PG) extract, the stabilized nanoparticles show significant changes in their respective vibrational spectra.

The interaction of Ag nanoparticles with biomolecules of (PG) showed intense peaks at 2935, 1629, 1515, 1384, 1156, 1076 and 1307 cm^{-1} relative shift in position and intensity distribution were confirmed by FT-IR (Fig. 2A and B) recorded for dry powder of (PG), where the strong bands were observed in 1702, 1622 and 1446 cm^{-1} . Comparing both FT-IR spectra it can be identified that the changes in the –COOH group for –OH, i.e., hydroxyl group the peak appeared at 3421 cm^{-1} in raw material, but after encapsulation of nanoparticles, the peak is narrower and shifted to 3391 cm^{-1} and also for –C– of carboxylic group the peak intensity reduced after encapsulation of nanoparticles. The band appearing at 1384 cm^{-1} corresponds to C–N stretching of amine group

[36] and in the raw extract the peak was broad and blend, but after encapsulation of nanoparticles the peak was narrow and sharper. This implies that –COOH group in the compound is attached to the gold nanoparticles and there in a clear change in the spectra. 1702 cm^{-1} in –C– bond stretching after the encapsulation this stretching is masked or disappeared.

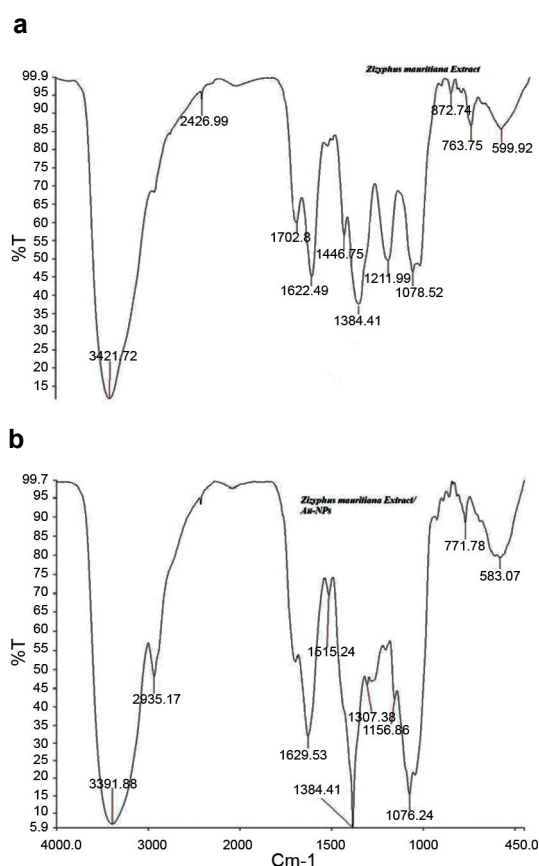


Fig. 2. FTIR spectra of *Psidium guajava* (PG) fruit powder (a) before and after (b) reaction.

The absorption peak at 3421 cm^{-1} observed in control extract, which is due to OH stretching vibration, get wider and shifted to 3391 cm^{-1} . This peak was assigned to the N–H group from protein present in the control extract. The N–H vibrational bands become weaker and broader in the spectrum of stabilized Ag nanoparticles. The IR bands at 1702 and 1622 cm^{-1} are characteristic of amide I whereas the band at 1515 cm^{-1} is characteristic of amide II respectively [8, 37–39]. In Fig. 2B, the two IR peaks of amide I were merged in one peak centered at 1629

cm^{-1} . These structural changes indicated that the reduction and stabilization of silver nanoparticles proceed via the coordination between N of the amide group and silver ions. The FTIR studies have confirmed the fact that the amide group forms proteins has the strong ability to bend metal indicating that the proteins could possibly form a layer covering the metal nanoparticles (i.e., capping of silver nanoparticles) to prevent agglomeration and thereby stabilize the medium. Comparison between spectra of the untreated sample to the treated samples Ag-NPs reveal only minor changes in the positions as well as to the magnitude of the absorption bands; wave numbers varying typically about $\pm 1-10 \text{ cm}^{-1}$.

TEM

The morphology and size of the synthesized silver nanoparticles were determined by TEM images and they are shown in Fig. 3(A and B).

The particles formed were spherical in shape. The nanospherical formed where shown to have high surface area. The nanoparticles formed were in the range of 15–25 nm in size with 36 nm average size. The particles were monodisperse, with only a few particles of different size [40–42].

SEM

Scanning electron microscopy (SEM) is used for morphological characterization at the nanometer to micrometer scale. SEM micro-graphs show aggregates of silver nanoparticles and the particles are in the range of 20–50 nm and there are not in direct contact even within the aggregates indicating the stabilization of nanoparticles by capping agents (Fig. 4A). In EDAX strong signals were observed from the silver atoms in the nanoparticles and weaker signals for carbon, oxygen, potassium and chloride were provenients from biomolecules of (PA) (Fig. 4B).

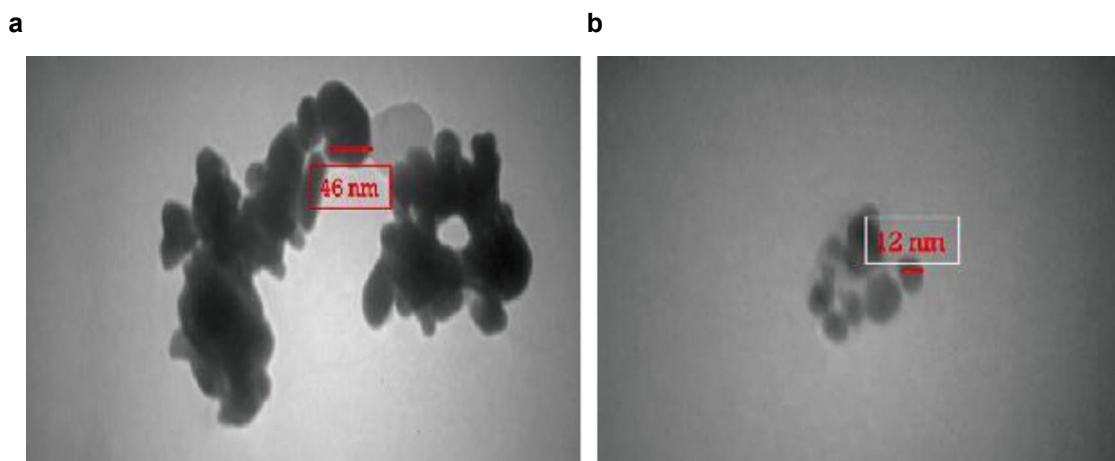


Fig. 3. TEM images indicating the presence of spherical silver nanoparticles recorded at various magnifications (a and b).

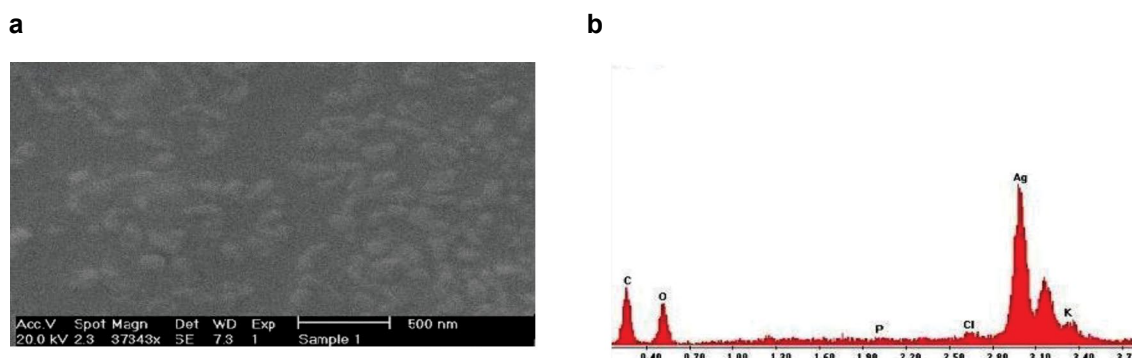


Fig. 4. (a) SEM and (b) EDAX images showing the presence of silver nanoparticles and bioorganic components of *Psidium guajava* (PG).

XRD

The crystalline nature of Ag-NPs was carried out using XRD where three diffraction peaks were observed in the 2θ range of $30\text{--}80^\circ$, which can be indexed as (1 1 1), (2 0 0), (2 2 0), (311) reflections of fcc structure metallic silver respectively similar to Joint Committee on Powder Diffraction Standards (JCPDS) file no: 04- 0784 revealing that synthesized Ag-NPs are of pure crystalline silver. The XRD patterns in (Fig. 5) of Ag-NPs obtained were similar to the results reported earlier [36, 43] The particle size of the Ag-NPs formed were calculated using Debye–Scherrer equation which was around 31 nm, were good in agreement with TEM results also.

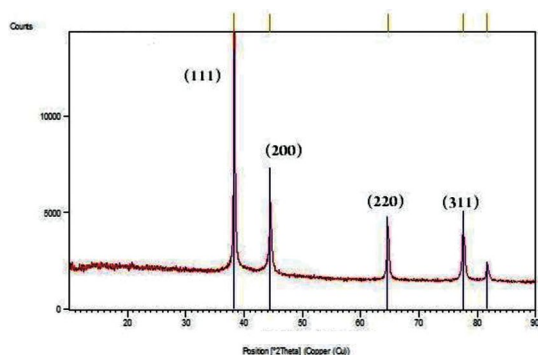


Fig. 5. XRD pattern of silver nanoparticles obtained using *Psidium guajava* (PG).

Antibacterial activity of silver nanoparticles

We have investigated the use of these (PG) mediated silver nanoparticles as possible antibacterial agents. Such (PG) mediated silver nanoparticles were immediately tested for antimicrobial activity towards test bacterial strains. Fig. 6A and B shows the zones of inhibition that were observed with the *S. aureus*. In all these figures, the black arrows indicate the *S. aureus* colonization. This is consistent with an earlier report on the antimicrobial activity of silver nanoparticles biosynthesized [44], as well as those synthesized chemically [24, 25]. In the present study, the nanoparticles thus synthesized could also be applied as selective antibacterial agents. The inhibition was observed in the Ag-NPs against *S. aureus*. The results suggest that the synthesized Ag-NPs act as an effective antibacterial agent.

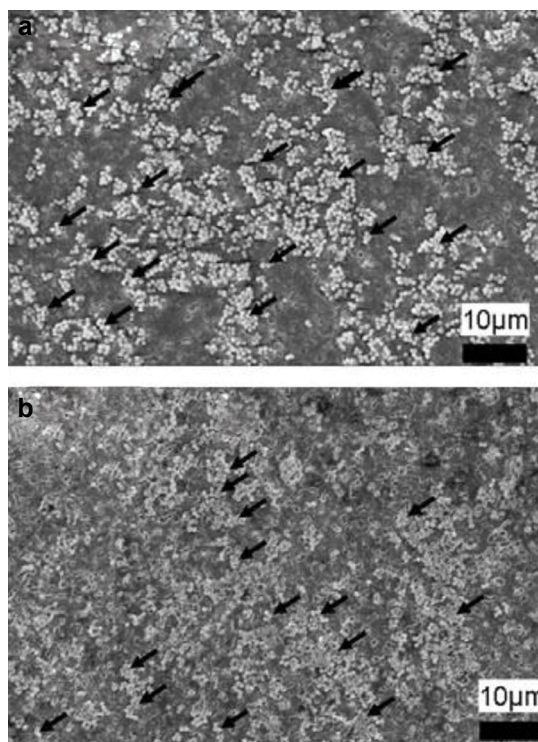


Fig. 6. Representative SEM images showing reduced *S. aureus* colonization on Ag-Nps/extract (b) compared to extract (a). Arrows show bacteria.

Stability of the synthesized Ag-NPs

Stability of bio-synthesized Ag-NPs was evaluated with zeta potentiometer at different pH after the synthesis of the metal nanoparticles (Fig. 7). It can be noted that synthesized Ag-NPs were stable in a wider range of pH from 7 to 11. With increase in pH, the value of zeta potential of Ag-NPs increases from $(-21.7$ to -64.3 mV). It was notable that Ag-NPs found stable in pH range from 7 to 11 (ZP value varied from -56.9 to -64 mV) but pH 11 found more stable. fruit extract mediated synthesized Ag-NPs and have high negative zeta potential values and thus they are stable under a wide pH range.

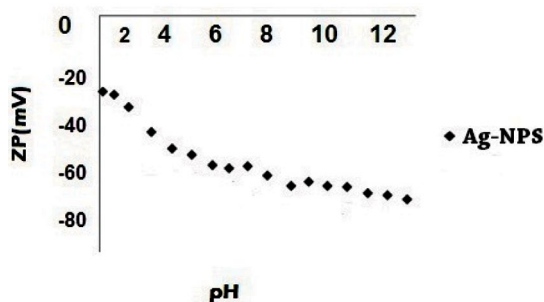


Fig. 7. Zeta potential at different pH.

CONCLUSION

In conclusion, the plant extract based synthesis can provide nanoparticles of a controlled size and morphology. The Ag-NPs were produced by the use of the extract of *psidium guajava* (PG) as reducing and capping agent. In this study, it was observed that the reaction is rapid and is completed within 35 min at room temperature. We have demonstrated an eco-friendly, rapid green chemistry approach for the synthesis of Ag-NPs by using (PG), which provides a simple, cost effective and efficient way for the synthesis of Ag-NPs. Therefore, this reaction pathway satisfies all the conditions of a 100% green chemical process. The amount of plant material was found to play a critical role in controlling the size and size dispersity of nanoparticles in such a way that smaller silver nanoparticles and narrow size distribution are produced when more (PG) extract is added in the reaction medium. The present study showed an innovative way of synthesizing antimicrobial Ag-NPs using natural products which can be used in various biomedical applications. Thus, the synthesized Ag-NPs could have a high potential for use in biological applications. The results confirmed that the (PG) is a very good Eco friendly and nontoxic source for the synthesis of Ag-NPs as compared to the conventional chemical/physical methods.

ACKNOWLEDGMENT

The financial and encouragement support provided by the Research vice Presidency of Tonekabon Branch, Islamic Azad University, Tonekabon, and Executive Director of Iran-Nanotechnology Organization (Govt. of Iran).

CONFLICT OF INTEREST

The authors declare that there is no conflict of interests regarding the publication of this manuscript.

REFERENCES

1. Y. Sun, B. Mayers, T. Herricks, Y. Xia, Nano Lett. 3 (2003) 955.
2. H. Srikanth, R. Hajndl, C. Chirinos, J. Sanders, Applied Physics Letters 79 (2001) 3503.
3. M Valle-Orta, D Díaz, P Santiago, E Reguera, A Vázquez-Olmos, Journal of Physical Chemistry 2008 (B 112) 14427.
4. L. Guo, Q. Huang, X. Li, S. Yang, Phys. Chem. Chem. Phys. 3 (2001) 1661.
5. A. Alqudami and S. Annapoorni, Plasmonics 2, 7 (2007) 5.
6. S.S. Shankar, A. Rai, A. Ahmad, M.Sastry, J.Colloid Interface Sci. 275 (2004) 496.
7. N. Duran, P.D. Marcato, G.I.H. De Souza, O.L. Alves, E. Esposito, J. Biomed. Nanotechnol. 3 (2009) 1.
8. J. Xie, J.Y. Lee, D.I.C. Wang, Y.P. Ting, Small 3 (2007) 672.
9. Y. Zhou, W. Chen, H. Itoh, K. Naka, Q. Ni, H. Yamane, Y. Chujo, Chem. Commun. (2001) 2518.
10. X. Zhai, S. Efrima, J. Phys. Chem. 100 (1996) 10235.
11. M.A. El-Sayed, Acc. Chem. Res. 34 (2001) 257.
12. A. Šileikaite, I. Prosyčevas, J. Puišo, A. Juraitis, A. Guobiene, Mater. Sci. 12 (2006) 287.
13. I. Sondi, B. Salopek-Sondi, J. Colloid Interf. Sci. 275 (2004) 177.
14. G.A. Sotiriou, S.E. Pratsinis, Sci. Technol. 44 (2010) 5649.
15. J. Huang, G. Zhan, B. Zheng, D. Sun, F. Lu, Y. Lin, H. Chen, Z. Zheng, Y. Zheng, Q. Li, Ind. Eng. Chem. Res. 50 (2011) 9095.
16. L. He, S. Gao, H. Wu, X. Liao, Q. He, B. Shi, Mater. Sci. Eng. C 32 (2012) 1050.
17. S. Kaviya, J. Santhanalakshmi, B. Viswanathan, J. Muthumary, K. Srinivasan, Spectrochim. Acta Part A 79 (2011) 594.
18. E.K. Elumalai, T.N.V.K.V. Prasad, J. Hemachandran, S.V. Therasa, T. Thirumalai, E. David, J. Pharm. Sci. Res. 2 (2010) 549.
19. M. Safaepour, A.R. Shahverdi, H.R. Shahverdi, M.R. Khorramizadeh, A.R. Gohari, J. Med. Biotechnol. 1 (2009) 111.
20. K. Kalishwaralal, V. Deepak, S.R.K. Pandian, M. Kottaisamy, S.B. Manikanth, B. Kartikeyan, S. Gurunathan, Colloid. Surface. B 77 (2010) 257.
21. M.N. Nadagouda, G. Hoag, J. Collins, R.S. Varma, Cryst. Growth Des. 9 (2009) 4979.
22. M.A.S. Sadjadi, Babak Sadeghi, M. Meskinfam, K. Zare, J. Azizian, Physica E: Low-dimensional Systems and Nanostructures, 40 (2008) 3183.
23. Babak Sadeghi, M.A.S. Sadjadi, R.A.R. Vahdati, Superlattices and Microstructures 46 (2009) 858.
24. Babak Sadeghi, M. Jamali, Sh. Kia, A. Amini Nia, S. Ghafari, Int. J. Nano Dimens. 1 (2010) 119.
25. Babak Sadeghi, Farshid S.Garmaroudi, M. Hashemi, H.R. Nezhad, A. Nasrollahi, Sima Ardalani, Sahar Ardalani, Advanced Powder Technology 23 (2012) 22.
26. Babak Sadeghi, A.Pourahmad, Advanced Powder Technology 22 (2012) 669.
27. Babak Sadeghi, Sh. Ghammamy, Z. Gholipour, M. Ghorchibeigy, A. Amini Nia, Mic & Nano Letters. 6 (2011) 209.
28. Babak Sadeghi, Spectrochimica Acta Part A: Molecular and Biomolecular Spectroscopy 118 (2014) 787.
29. Babak Sadeghi, M. Meskinfam, Spectrochimica Acta Part A: Molecular and Biomolecular Spectroscopy 97 (2012) 326.
30. B. Umesh, J.Vishwas, A.Bapat, Industrial Crops and Products 46 (2013) 132.
31. Q.L. Feng, J. Wu, G.Q. Chen, F.Z. Cui, T.N. Kim, J.O. Kim, J. Biomed. Mater. Res. 52 (2000) 662.
32. A. Melaiye, Z. Sun, K. Hindi, A. Milsted, D. Ely, D.H. Reneker, C.A. Tessier, W.J. Youngs, J. Am. Chem. Soc. 127 (2005) 2285.

33. W.K. Son, J.H. Youk, T.S. Lee, W.H. Park, *Macromol. Rapid Commun.* 25 (2004) 1632.
34. M.Sastry, K.S.Mayyaa, K.Bandyopadhyay, *Colloids Surf. A* 127 (1997) 221.
35. X. Wang, G.J. Bunkers, *Biochem. Biophys. Res. Commun.* 279 (2000) 669.
36. K. Badri Narayanan, N. Sakthivel, *Mater. Lett.* 62 (2008) 4588.
37. S. He, Y. Zhang, Z. Guo, N. Gu, *Biotechnol. Prog.* 24 (2008) 476.
38. D.S. Sheny, Daizy Philip, Joseph Mathew, *Spectrochim. Acta A* 91 (2012) 35.
39. S. Basavaraja, S.D. Balaji, A. Lagashetty, A.H. Rajasab, A. Venkataraman, *Mater. Res. Bull.* 43 (2008) 1164.
40. A.Kumar Mittal, Y.Chisti, U.Chand Banerjee. *Biotechnology Advances* 31 (2013) 346.
41. A.S. Eppler, G. Rupprechter, E.A. Anderson, G.A. Somorjai. *J.Phys.Chem.B.* 104 (2000) 7286.
42. S. S,Shankar, A. Rai, A .Ahmad, M. Sastry. *J Colloid Interface Sci.* 275 (2004) 496.
43. K. Badri Narayanan, N. Sakthivel, *Mater. Lett.* 62 (2008) 4588.
44. Chaloupka K, Malam Y, Seifalian AM. *Trends Biotechnol* 28 (2010) 580.